2005-05-20

An Improved MUSIC Model for Gibbsite

Scott Christian Mitchell

Brigham Young University - Provo

AN IMPROVED MUSIC MODEL FOR GIBBSITE

by

Scott C. Mitchell

A thesis submitted to the faculty of

Brigham Young University

in partial fulfillment of the requirements for the degree of

Master of Science

Department of Geology

Brigham Young University

August 2005

BRIGHAM YOUNG UNIVERSITY

GRADUATE COMMITTEE APPROVAL

of a thesis submitted by

Scott C. Mitchell

This thesis has been read by each member of the following graduate committee and by majority vote has been found to be satisfactory.

_____   _____
Date   Barry R. Bickmore, Chair

_____   _____
Date   Dana T. Griffen

_____   _____
Date   James P. Lewis

BRIGHAM YOUNG UNIVERSITY

As chair of the candidate's graduate committee, I have read the thesis of Scott C. Mitchell in its final form and have found that (1) its format, citations, and bibliographical style are consistent and acceptable and fulfill university and department style requirements; (2) its illustrative materials including figures, tables, and charts are in place; and (3) the final manuscript is satisfactory to the graduate committee and is ready for submission to the university library.

_____   _____
Date   Barry R. Bickmore
                                        Chair, Graduate Committee

Accepted for the Department

                                        _____
                                        Bart J. Kowallis
                                        Graduate Coordinator

Accepted for the College

                                        _____
                                        G. Rex Bryce
                                        Dean, College of Physical and Mathematical
                                        Sciences

ABSTRACT

AN IMPROVED MUSIC MODEL FOR GIBBSITE

Scott C. Mitchell

Department of Geology

Master of Science

Several recent studies that have proposed MUSIC models for gibbsite surfaces
have purported to achieve a very good fit with potentiometric titration data. However, in
order to achieve such results, several significant parameters, such as the number of
surface sites, site densities, and pK_a values were sometimes re-introduced in the model as
fitted parameters, and physically unrealistic modeling assumptions were sometimes used.
In addition, recent evidence supports the idea that some of the gibbsite potentiometric
titration data from these studies may be unreliable. In order to re-interpret the
potentiometric titration data, we used several recently published methods. In order to
detect possible problems with estimates of gibbsite basal and edge surface area, we
synthesized two gibbsite samples with different aspect ratios and characterized their
surface areas using BET, AFM, and computerized image analysis routines. We also
estimated pK_a values for acid/base reactions at gibbsite surfaces by applying a new bond-
valence method to gibbsite (001)-type and (100)-type surface structures based on *ab*

initio calculations. The resulting pK_a estimates are not to be taken as precise values due to difficulties and assumptions associated with calculating reasonable *ab initio* surface structures. Instead, we believe they represent a more reasonable range than has been previously estimated. Using these estimates, we propose an improved MUSIC model for gibbsite, which seems to predict surface adsorption, not perfectly, but within a reasonable range for a number of titration data sets without re-introducing any of our estimated parameters as adjustable parameters. Discrepancies that exist between model predictions and various potentiometric titration data sets are likely due to error associated with potentiometric titrations and pK_a predictions.

ACKNOWLEDGMENTS

TABLE OF CONTENTS

LIST OF TABLES

LIST OF FIGURES

INTRODUCTION

Adsorption at mineral surfaces plays an important role in both agricultural and environmental science because many reactions between soils and aqueous solutions, and all reactions between rocks and aqueous solutions, involve mineral surfaces. These reactions affect life-sustaining processes such as plant nutrition and growth, as well as life-threatening processes such as contaminant transport. As a result, soil science and environmental science require an accurate knowledge of mineral surface adsorption behavior in order to understand processes important to the health of our environment and the development of our resources.

In the field of mineral surface chemistry, gibbsite ($Al(OH)_3$) is important for several reasons. First, it is relatively ubiquitous in soil systems and has a large surface area, thus giving it high potential for surface adsorption. It is a platy, pseudo-hexagonal mineral dominated by a basal (001)-type crystal face and two edge ((100)-type and (110)-type) crystal faces. Only doubly coordinated $>Al_2OH$ surface sites are present on the (001) face at a density of 13.7 nm^{-2}. On the (100)-type and (110)-type faces $>Al_2OH$ sites are present along with singly coordinated $>AlOH$ sites, each at a density of 8.1 nm^{-2}. Gibbsite is also the mineral on which a popular surface complexation model was calibrated (Heimstra et al., 1989; 1996) and, as such, has been the subject of numerous modeling studies.

The purpose of surface complexation models (SCMs) is to describe the adsorption behavior of mineral surfaces. While these models can be helpful for understanding adsorption behavior qualitatively, they often fail to provide reliable information at the molecular scale. This is because there are too many adjustable parameters in the models.

Surface complexation modelers can fit Helmholtz layer capacitances, surface equilibrium constants, and number of surface sites. In addition, these models treat surfaces as planes of uniform charge and assume the presence of only one type of surface site, even though this is often not the case. As a result, surface complexation modeling can become an exercise in curve-fitting with little basis in molecular-scale reality.

Heimstra et al. (1989; 1996) developed the multi-site complexation (MUSIC) model for use with oxide surfaces as an improvement on traditional SCMs. This model brought much-needed reforms to surface complexation modeling by requiring that a number of previously adjustable parameters be constrained experimentally or theoretically, distributing charge more realistically over surfaces, and accounting for multiple site types. As a result, the MUSIC model attempts to provide some of the molecular scale detail lacking in traditional SCMs.

The MUSIC model requires that surface site types, site densities, areas of crystallographically distinct surfaces, and equilibrium constants be constrained. Microscopic imaging methods are used to constrain surface areas of crystallographically distinct surfaces, while site densities are calculated from crystallographic models. These parameters are then used together to constrain the number of surface sites of each type available for adsorption. Equilibrium constants are constrained in a slightly more complicated way. First, the valence at each surface site must be calculated. Valence can be described as a measure of the valence electron states associated with a bond. The first step in calculating valence is to cut a theoretical surface through a bulk gibbsite structure, making sure to terminate the surface on O atoms, and measuring the Al-O bond lengths

for each surface site. The relationship between bond length and bond valence is described empirically by the following equation (Brown and Altermatt, 1985)

$$s = \exp\left[\frac{R_0 - R}{B}\right],$$ (1)

where s is bond valence in valence units (v.u.), R is bond length (Å), and R_o and B are parameters specific to a given cation-anion pair. For each surface oxygen, the valence associated with Al-O bonds reaching the O atom (s_{Al}) can be calculated using Eqn. 1. Valence associated with O-H bonds must also be accounted for. The valence of each O-H bond (s_H) is assumed to be 0.8 valence units (v.u.) (Hiemstra et al., 1996; Brown, 2002; Bickmore et al., 2003). The number of O-H bonds reaching the O atom is represented by the variable m. Finally, valence associated with weak hydrogen bonding is assumed to be 0.2 v.u. (Hiemstra et al., 1996; Brown, 2002; Bickmore et al., 2003). The number of weak hydrogen bonds reaching an O atom (n) is equal to the total number of proton docking sites, less those already occupied by Al-O or O-H bonds. The total number of proton docking sites is assumed to be 4, but for surface functional groups, sometimes one of the docking sites is assumed to be sterically hindered from reacting. Total bond valence for the O atom can then be determined using the equation

$$s_t = s_{Al} + ms_H + n(1 - s_H),$$ (2)
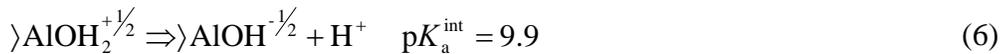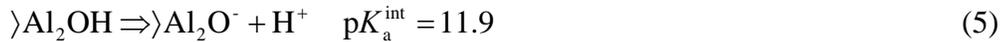
where s_t is the total valence of bonds reaching the O atom. Intrinsic acidity constants for surface O sites are then predicted from s_t using the following empirical relationship

$$pK_a = A(s_t + V),$$ (3)

where $A = -19.8$, s_t is calculated using Eqn. 2, and V is the formal charge of the O atom (-2). Since equilibrium constants for individual surface sites cannot be determined

experimentally, this empirical formula was calibrated on the structures and known acidities of a number of (hydr)oxy-acid solution monomers.

Heimstra et al. (1999) used these methods to predict surface properties of gibbsite. They predicted the following pK_a values for the deprotonation of gibbsite surface sites

$$\rangle Al_2OH_2^+ \Rightarrow \rangle Al_2OH + H^+ \quad pK_a^{int} = 0 \tag{4}$$

$$\rangle Al_2OH \Rightarrow \rangle Al_2O^- + H^+ \quad pK_a^{int} = 11.9 \tag{5}$$

$$\rangle AlOH_2^{+\frac{1}{2}} \Rightarrow \rangle AlOH^{-\frac{1}{2}} + H^+ \quad pK_a^{int} = 9.9 \tag{6}$$

These predictions suggest that only the singly coordinated surface sites on gibbsite edges are reactive in the environmental pH range (about pH 3-11) and the point of zero net proton charge (PZNPC) for gibbsite should be 9.9. Potentiometric titrations performed in the study also showed the PZNPC at about 10, and measured surface charge seemed to correlate fairly well with the proportion of edge surface area in the samples studied.

Nevertheless, the ability of MUSIC modeling to provide a realistic picture of surface adsorption on gibbsite surfaces is questionable. Most MUSIC models for gibbsite do a fair job predicting surface charge for one or two samples. However, they are often created using unrealistic assumptions and they usually fail when applied to multiple data sets or sample types. The two main causes of MUSIC model failure are difficulty in data collection and the re-introduction of fitted parameters. For example, Heimstra et al. (1999) created a MUSIC model for gibbsite and compared it with potentiometric titration data collected using two-minute titration steps. The model predicted surface charge for three of their four samples fairly well. However, for surface charge data from another study using 20-minute titration steps (Kavanagh et al., 1975), surface charge was too high to be accounted for by the available singly coordinated edge sites. To account for this

phenomenon, Kavanagh et al. (1975) re-introduced the number of surface sites as an

adjustable parameter by suggesting the presence of singly coordinated sites as defects on

the basal surfaces. In another study of gibbsite surfaces, Rosenqvist et al. (2002) used

titration data collected using 8-14 hour titration steps to ensure adequate pH equilibration.

However, when they tried to apply the model of Hiemstra et al. (1999), their surface

charge data was much higher than model predictions. Therefore, they re-introduced

equilibrium constants as adjustable parameters by proposing a co-adsorption mechanism

of hydrogen and chloride ions to the doubly coordinated basal surface sites. The

equilibrium constant for this mechanism was not estimated theoretically, but rather

adjusted to make their model fit the data. While fitting electrolyte binding constants in

this way is common, the magnitude of the fitted constant is usually small enough that it

does not dominate model predictions. In the model of Rosenqvist et al. (2002), however,

the binding constants were as large as 8.49 log units and shifted model predictions

considerably. One thing that Rosenqvist et al. (2002) did correctly was to treat gibbsite

basal and edge surfaces as distinct surfaces in their model, as opposed to others who

included all surfaces sites on a single surface. Finally, Jodin et al. (in press) disagreed

with the use of 8-14 hour titration steps, citing concerns with gibbsite dissolution at low

pH, and used 10-minute titration steps. Two-second, time resolved pH analysis

suggested that pH was adequately equilibrated after 10 minutes. The resulting surface

charge was similar in magnitude to that of Kavanagh et al. (1975). Although they did not

create a complete MUSIC model for their study, they did re-estimate pK_a values. Again,

this involved some arbitrary adjustment. Specifically, they adjusted the total number of

available proton docking sites and s_H values on some surface oxygens. Interestingly,

adjusting the number of available proton docking sites is explicitly allowed in MUSIC modeling, even though there is no theoretical justification for doing so. Essentially, this is simply a way to adjust individual pK_a estimates by 4 log units in either direction (see Eqns. 2-3).

A number of recent publications have attempted to determine the limitations of the MUSIC model and to improve its reliability for use with gibbsite. Jodin et al. (in press) emphasized that surface charge data of gibbsite has been characterized only within a very large range because of the experimental uncertainty associated with potentiometric titrations. Bickmore et al. (2004) emphasized the need for, and proposed an improved method of, pK_a prediction that takes non-ideal electrostatic factors and bond relaxation into account. Bickmore et al. (2002) and Jodin et al. (2004) also concluded that methods previously used for quantifying edge and basal surface area are flawed. The use of methods introduced by both papers have been much more successful at producing reliable estimates. However, to date, no study has incorporated the use of these improved methods to create a MUSIC model for gibbsite.

Our goal in this study is to account for the gibbsite potentiometric titration data mentioned above by 1) determining which data sets are most reliable, and 2) creating an improved MUSIC model for gibbsite using the new pK_a prediction method of Bickmore et al. (2004) and more robust methods of surface equilibrium modeling than have normally been used in the past. This should result in a reasonable fit of titration data while maintaining a physically realistic model and the fewest possible fitted parameters.

METHODS

In order to re-interpret potentiometric titration data from the studies mentioned above, the following issues must be addressed: 1) titration data collection, 2) surface area estimates, 3) pK_a prediction, and 4) surface equilibrium modeling methods. Titration data collection will be addressed in the Results and Discussion section below. Problems with surface area estimates for gibbsite have been discussed by Jodin et al. (2004). However, their sample contained much larger particles and had lower surface area than samples used in other studies. Therefore, we synthesized gibbsite samples similar to those used in other studies and performed surface area analysis on them. In order to obtain reasonable pK_a estimates, we analyzed *ab initio* surface structures using the method of Bickmore et al. (2004). For surface equilibrium modeling we used software capable of treating crystallographically distinct surfaces on mineral particles as spatially separate.

Gibbsite Preparation

Gibbsite was synthesized by titration of 4M NaOH into 500 mL of 1M AlNO$_3$ at a rate of 10 mL/min. When the solution reached pH 4.5 amorphous aluminum hydroxide Al(OH)$_3$ precipitated as a gelatinous slurry. The slurry was transferred into dialysis tubing and placed into 1L plastic containers, which were subsequently filled with de-ionized water, sealed tightly, and placed in constant temperature water baths for various

periods of time. The de-ionized water was replaced six days a week to insure adequate

dialysis and gibbsite purity.

We synthesized gibbsite samples with different aspect ratios (i.e. different

proportions of edge and basal surface area, similar to those prepared by Hiemstra et al.

(1999)).   Sample H (high temperature) was crystallized at 70ºC for 12 weeks. Sample L

(low temperature) was crystallized at 4ºC for eight weeks and then placed in the 70ºC

bath for an additional eight weeks to increase crystallinity. After the crystallization time

was completed for each sample, the suspension was freeze-dried, resulting in a very fine,

white, gibbsite powder. Gibbsite crystallized under the conditions used to synthesize

sample L should exhibit a different aspect ratio than gibbsite crystallized under

conditions used to synthesize sample H (Figure 1) (Hiemstra et al., (1999).

X-Ray Photoelectron Spectroscopy (XPS)

Synthesized mineral surfaces can sometimes become contaminated during the

synthesis process, which can affect crystal growth morphology, and hence, surface area

estimates. The most likely contaminant for gibbsite surfaces is silica, which can dissolve

out of laboratory glass at high pH (Kosmulski, 2003). Although we were careful to avoid

contamination and no glass was used in gibbsite synthesis, we used x-ray photoelectron

spectroscopy (XPS) to double-check our sample surfaces for purity. XPS analysis was

performed using an SSX-100 ESCA Spectrometer (Surface Science Instruments).

Powder X-Ray Diffraction (XRD)

It was important for our samples to be well crystalline in order to accurately estimate total surface area and differentiate between basal and edge surfaces. We used a powder x-ray diffractometer (XRD) to check for well-defined gibbsite peaks and to ensure that no other crystalline phases were present. XRD was performed on powder samples using an XDS 2000 diffractometer (Scintag Inc., Cupertino, California).

Surface Area Analysis

In order to obtain estimates of total surface area and percent edge surface area for each sample, we used two analytical methods. First, we used BET analysis to measure total surface area. The BET method gives accurate measurements of total sample surface area within about ±10%. We used a Gemini 2360 Surface Area Analyzer (Micromeritics, Norcross, Georgia) with 11 analysis points and a pressure equilibration time of 5 minutes.

However, BET is not capable of differentiating between edge and basal surface area, a distinction that is necessary in order to quantify the distribution of surface functional groups in a sample. In order to accurately estimate basal and edge surface areas we used Atomic Force Microscopy (AFM) and computerized image analysis routines developed by Bickmore et al. (2002). We used a Nanoscope IIIa Multimode AFM (Digital Instruments, Santa Barbara, California) in TappingMode® for the analysis. Samples were prepared by dispersing a few small flakes of gibbsite powder in 1L of pH 3.5 HCl, which was then covered and magnetically stirred for 48 hours. Samples

prepared in solutions with pH much higher than 3.5 exhibited edge to basal surface particle clumping and edge to mica surface orientation under the AFM and could not be analyzed using these routines. After 48 hours, the suspension was sonicated for five minutes and a drop was flash boiled on a freshly cleaved mica flake that had been heated on a hot plate at 400ºC. This method of preparation usually results in a good dispersion of particles on the slide, which is necessary to ensure unbiased sampling.

We imaged particles from each sample and discovered that particles had a bi-modal size distribution, making it more difficult to image large numbers of particles at the same time (Figure 2). This difficulty arises because when small and large particles are present in the same scanned image, small particles cannot be imaged to a sufficient level of detail. It is necessary, however, to analyze a large enough number of particles in their natural distribution on the slide to obtain a statistically accurate estimate of surface area. Therefore, we reduced the scan size to < 1 µm and imaged a sample of between 48 and 67 small particles. After creating histograms of specific surface area to determine that our small-particle sample had a distribution that was representative of all small particles, we increased the scan size to between 4 – 20 µm to image the large particles. When the large particles were imaged, small particles interspersed among them were counted. The total number of small particles counted in these scans was divided by the number of particles in the small-particle sample group to determine how many times the small-particle sample group had to be counted to estimate specific surface area.

Particle images were analyzed using computerized image analysis routines programmed in the Image SXM image analysis environment (Bickmore et al., 2002). The macros use particle perimeter measurements at 256 height levels to calculate total

specific surface area and percent edge surface area. The main advantage of this method is that it accounts for the microtopography that exists on particle surfaces. Assuming the bottom half of a particle is a mirror image of the top also corrects for microtopography that AFM is unable to image on the bottom of a particle.

Edge surface area was not divided into (100)-type and (110)-type type surface area during AFM imaging and analysis. Rather, we assumed that 2/3 of the edge surface area was (110)-type type surface and 1/3 was (100)-type type surface because of the pseudo-hexagonal shape of gibbsite particles and the orientation of each surface (Figure 1).

Acidity Constant Estimates

Estimates of surface site acidity constants were calculated using *ab-initio* surface structure optimizations and a new bond-valence method developed by Bickmore et al. (2004). Optimized bulk, surface, and edge structures were calculated using the pseudopotential plane wave density functional theory method as implemented in CASTEP (Payne et al., 1992). The approach applied here is, for the most part, identical to that which was reported previously (Rosso et al., 2001; Bickmore et al., 2003; Bickmore et al., 2004). Thus, only new details pertinent to the current calculations will be described here. The generalized gradient approximation (GGA) was applied using the Perdew-Wang (Perdew and Wang, 1992) parameterization of the exchange-correlation functional, modified to work with plane wave calculations (White and Bird, 1994). We used the CASTEP parameterization of ultrasoft pseudopotentials (Vanderbilt, 1990) without core corrections. Optimization was performed using a cutoff energy of 380 eV

and a conjugate gradient electronic minimizer using a density mixing scheme (Kresse and Furthmuller, 1996). One k-point was used (gamma point). Cell parameters and atomic coordinates of the bulk structures were optimized without symmetry restrictions (i.e., P1 symmetry).

Because these calculations always have three-dimensional periodic boundary conditions, surfaces were constructed by building in a vacuum layer (Rosso, 2001). The (100)-type and (110)-type surfaces are edge surfaces of octahedral sheets, and were modeled as polymer-like repeat units one sheet thick. Hence, in these edge models two mutually perpendicular vacuum layers were present. The (001) surface is the basal surface, and was modeled using three octahedral sheets. Vacuum layers were no less than approximately 8 Å wide. Protons were added to or subtracted from oxygen atoms at the (100)-type and (110)-type edges and the (001) basal surface in various configurations to be included in the all-atom optimizations, as will be discussed in more detail below in the Results and Discussion section. The slab models were optimized with fixed unit cell parameters, which were supercells based on the optimal bulk unit cell parameters. Various numbers of protons were added to the surface to investigate bond length dependencies on protonation states. Some proton configurations yielded a charge neutral unit cell; others did not. For the latter, the uniform background charge method was used to neutralize the unit cell.

The surface groups on the optimized structures were analyzed using the method of Bickmore et al. (2004). This method uses Al-O bond lengths and bond ionicity to estimate the pK_a of oxide surface groups with the following empirical relationship

$$pK_a^{int}(\pm 0.83) = 61.5S_b + 22.5I + 19.2 \tag{7}$$

where S_b is the "Lewis base strength" of the O atom from which a proton has been removed in an acid dissociation reaction and is calculated by dividing the unsaturated valence $(s_t + V)$ of the O atom (see Eqns. 2-3) by the number of docking sites not taken up by Al-O or O-H bonds. I is the fraction ionic character of the Al-O bond calculated with the following equation

$$I = 1 - \exp\left[-\frac{(X_A - X_B)^2}{4} \right] \tag{8}$$

where $(X_A - X_B)$ is the electronegativity difference between the metal and oxygen atoms (Pauling, 1960). The fraction ionic character of the Al-O bond in gibbsite is 0.567 (Bickmore et al., 2004).

Surface Complexation Modeling

Surface complexation modeling was performed using a modified version (Lützenkirchen, J., personal communication) of the computer code FITEQL 2.0 (Westall, J.C., 1982), coupled with the UCODE inverse modeling script (Poeter and Hill, 1998). This modified code allows up to nine distinct surfaces to be modeled simultaneously, and the UCODE script allows the model to be simultaneously fit to up to nine different data sets. In addition, we used a graphical user interface created by B.R. Bickmore in Microsoft Excel, which generates the necessary input files and extracts and graphs output from the modeling software.

Gibbsite typically exhibits three distinct surface types: (001), (100), (110), and their symmetric equivalents. The (100)-type and (110)-type surfaces are nearly identical in surface site type and site density. Because of their similarity and difficulties

13

calculating reliable surface structures for the (110)-type surface, which will be discussed below, we treated the (100)-type and (110)-type surfaces as equivalent in the model.

For our model we used the basic Stern framework. Activity coefficients for different ionic strengths were calculated with the Davies equation. The capacitance for the basal (001) surface was assumed to be different than the capacitance for the edge surfaces since its structure, site density, and charging behavior differs significantly. The same binding constant was used for both cations and anions in all model reactions.

RESULTS AND DISCUSSION

Sample Characterization

Sample characterization with XPS and XRD showed that our gibbsite samples were pure and well crystalline. XPS showed that no surface contamination was present other than some adventitious carbon. In addition, both samples showed O to Al ratios of 3.0:1.0. XRD showed well-defined diffraction peaks characteristic of gibbsite, with no others present.

Surface Area Characterization

We synthesized our gibbsite samples after samples from Heimstra et al. (1999) in order to compare sample characterization results. Our samples H and L correspond to samples GH2 and GL1 of Heimstra et al. (1999), respectively. BET results for the specific surface areas (SSA) of all samples are shown in Table 1 and suggest that the samples are indeed similar. The BET specific surface areas of sample H and sample GH2

match within the experimental error of the method. The BET specific surface areas of sample L and sample GL1 differ by about 10%.

As mentioned above, in order to create a MUSIC model it is necessary to differentiate between edge and basal surface area. Since the BET method measures only the total SSA, other methods must be used to do this. Ideally, the basal and edge surface area estimates obtained from these other methods should add up to equal the surface area estimate obtained by the BET method. Table 1 shows SSA estimates for gibbsite samples from several recent studies made using various other methods, compared to SSA estimates for the same samples based on BET. SSA estimates from this study using AFM images and analysis routines (Bickmore et al., 2002) matched SSA estimates based on BET within experimental error. The SSA estimates for samples GH2 and GL1 (Heimstra et al., 1999) from transmission electron micrographs (TEM) and platinum shadowing, on the other hand, are much higher than SSA estimates based on BET. Rosenqvist et al. (2002) reported an SSA estimate from AFM analysis that was significantly higher than the BET estimate. However, Jodin et al. (2003) nearly matched the Kr-adsorption estimate of their sample's SSA using the method of Bickmore et al. (2002). In the remainder of this section, we will discuss the results from each of these studies and suggest possible reasons for the differences in surface area estimates.

Attempts to accurately quantify basal and edge SSA have only been made recently and there is still significant work being done on the subject. In fact, each of the recent studies examined in this paper used different methods to calculate SSA estimates of platy particles and exhibited very different results. However, Bickmore et al. (2002) and Jodin et al. (2004) identified two crucial factors that must be accounted for in any

15

such method used on platy particles. First, the SSA must be normalized for mass to properly account for the larger effect of more massive particles on SSA in a heterogeneous sample. Second, the microtopography that exists on all particle surfaces must be taken into account. Microtopography may not be difficult to account for on surfaces that are easily imaged by microscopic methods, however, surfaces on the edge and bottom of particles are often difficult or impossible to image using these methods.

Accounting for these two factors can have a very large effect on SSA estimates. Table 2 shows how they affected the SSA estimates in this study. Estimates calculated using a number-averaged surface area (ASA) were 363% and 125% higher than BET values. This occurred because the small particles greatly outnumbered the large particles. Therefore, using an average resulted in an estimate more representative of small particles. However, despite the fact that the more massive particles are fewer in number, they dominate the SSA. Looking at it from another perspective, using number-averaged calculations to estimate SSA results in an estimate of surface area per number of particles. Yet, by definition SSA is defined as surface area per mass.

If we normalize the estimates for mass, but do not account for microtopography on particle bottoms, the results are much closer to those based on BET, but still lower by 15 - 42% (Table 2).

Only after normalizing for mass and correcting for microtopography on the bottoms of the particles (BCMNSA) do estimates match BET values within experimental error (Table 2). The bottom correction increased the estimated SSA by over 15 m^2/g for sample H, and by about 5 m^2/g for sample L.

Heimstra et al. (1999) reported SSA estimates based on TEM and platinum shadowing routines that differed significantly from estimates based on BET (Table 1). However, since they normalized for mass in their calculations, inaccuracies are likely due to two factors. First, their method was unable to accurately image and account for microtopography on the bottoms of particles. Second, they were not sure whether their sample was adequately dispersed, and may have treated growth features as separate particles. This would have increased their total surface area estimates.

Rosenqvist et al. (2002) reported estimates of SSA based on AFM image analysis that also differed significantly from estimates based on BET. This error can be attributed to the failure both to normalize their estimate for mass and to correct for microtopography on the bottoms of particles. Of these two failures, failure to normalize for mass probably had the largest effect on their estimates. We can illustrate the magnitude of this effect by referring again to Table 2. Number-averaged AFM estimates of SSA for samples H and L were 136 - 54 m^2/g higher than BET estimates, respectively. Therefore, it is completely reasonable that the discrepancy (62 m^2/g) between the number-averaged AFM estimate and the BET estimate of Rosenqvist et al. (2002) could be mostly attributed to the averaging effect.

The work of Jodin et al. (2004) reinforces the need to account for mass effects and particle microtopography. They were able to approximate their surface area estimates to results of Kr-adsorption and infrared spectroscopy using the method of Bickmore et al. (2002). They used both number-averaged and mass-normalized calculations to make several SSA estimates. When they used a weight-averaged summation of basal area, edge area, and volume and added a correction to account for bottom microtopography

17

they were able to approximate the Kr-adsorption value within 12%. As was the case with this study, number-averaged estimates were always much larger than gas adsorption results. In addition, mass-normalized estimates were also significantly smaller than gas adsorption estimates until corrections for particle microtopography were made. This should usually be the case for a heterogeneous sample of platy particles in which the small particles outnumber the large particles.

pK_a Prediction

We used the method of Bickmore et al. (2004), in conjunction with our calculated gibbsite surface structures to estimate surface pK_a values. Ideally, we would have started with completely deprotonated surfaces and estimated the pK_a values of each surface site. Then, the site with the highest pK_a would have been protonated and the surface would have been re-optimized. The pK_a values for the remaining deprotonated sites then would have been calculated again. This would have been repeated until each surface site was fully protonated. However, certain adjustments had to made to the method because of the sensitivity of the *ab initio* calculations to surface charge. Because of these adjustments the pK_a values reported here should only be taken as rough estimates.

Basal (001) Surface

The (001)-type basal surface of gibbsite consists only of doubly coordinated sites in the >Al2OH2+, >Al2OH, and >Al2O- forms. Because there are two deprotonation reactions, two pK_a values must be calculated for these groups (see the reactions in Eqns. 4-5). In order to calculate pK_a values for the first and second deprotonation reactions, the

Al-O bond lengths for each surface group must be calculated in the >Al2OH and >Al2O-

forms, respectively.

Since there are six of these doubly coordinated sites on the (001) surface per unit

cell, we calculated a total of twelve pK_a values for the (001)-type surface sites (Table 3).

The quantum mechanical code that was used, however, was very sensitive to surface

charge. When the surface charge was too high (greater than ±3) it was unable to

determine the absolute minimum energy configuration and, as a result, could not optimize

the structures. In order to avoid this problem, we estimated pK_a values for the first

deprotonation reaction from the neutral surface. In order to estimate pK_a values for the

second deprotonation reaction, we first removed protons from the three sites with the

lowest pK_a estimates for the first deprotonation reaction, resulting in a manageable

surface charge of –3. After optimizing this surface structure, we calculated the pK_a

estimates for these three sites. In order to estimate pK_a values for the second

deprotonation reaction on the remaining three sites, we added the average difference

between the pK_a values for the first and second deprotonation reactions (9.2 log units) on

the first three sites to the pK_a estimates for the first deprotonation reaction of the

remaining sites.

Based on our predicted pK_a values for these sites, the basal surface of gibbsite has

a point of zero net proton charge (PZNPC) of ~4.5. A PZNPC in this range is also

supported by experiments performed on the (001) surface of corundum/sapphire, which

also consists of only doubly coordinated aluminol groups. A number of studies have

used AFM force titrations and second harmonic generation experiments on these surfaces

to determine their PZNPC. The reported values ranged from pH 3 – 6.7 (Stack et al.,

19

2001; Franks and Meagher, 2003; Horn et al., 1988; Ducker et al., 1994; Larson et al., 1997; Meagher et al., 2002). Our predicted PZNPC of ~4.5 for gibbsite basal surfaces is, therefore, within the range of experimentally determined PZNPCs of similar surfaces.

Edge (100)-type and (110)-type Surfaces

Predicting pK_a values for edge surfaces also presented challenges. Edge surfaces contain singly and doubly coordinated surface sites in equal densities. However, the doubly coordinated sites are set deeper in the surface than the singly coordinated groups, which protrude from the surface (Figure 3). As a result, these doubly coordinated sites may be sterically hindered from reacting. Some of our surface structure optimizations suggest that this is a reasonable assumption. When we attempted to optimize surface structures in which the doubly coordinated sites were deprotonated, resulting surface structures were not reliable.   In addition, a recent study by Rustad et al. (2003) on magnetite surfaces concluded that physical isolation of certain surface sites from the solvent makes them non-reactive. In another study on goethite surfaces, surface sites at acute edges, which are more accessible to protons, were shown to be more likely than other sites to accumulate protons (Rustad et al., 2005). For these reasons, we assumed that the deeper-set doubly coordinated sites on gibbsite edges are not reactive and did not attempt to estimate pK_a values for them.

Another difficulty encountered was that the (110)-type surface unit cell was twice as long as that of the (100)-type surface. This resulted in the following problems. First, a larger surface with more surface sites can build up higher surface charge. As mentioned above, the quantum mechanical code that was used for these structures was unable to

optimize structures with a high surface charge. Second, the longer (110)-type surface

unit cell would require significantly more computing time unless the system were made

smaller by making the surface slab and vacuum layer thinner. This, however, can also

result in structures failing to optimize correctly.

In order to resolve these problems, we used the pK_a predictions from the (100)-

type surface for both edge surfaces in our models. Since the (110)-type and (100)-type

surfaces have the exact same surface groups in the exact same positions and in equal

densities, this seems to be a reasonable approximation. However, since the symmetry of

gibbsite is monoclinic and the (100)-type and (110)-type surfaces are not strictly identical

in a crystallographic sense, it is also reasonable to assume that some variance in pK_a may

exist between these surfaces. More work must be done in order to calculate a reliable

(110)-type surface structure.

Assuming that the doubly coordinated sites are not reactive, pK_a values for singly

coordinated sites on the (100)-type and (110)-type surfaces were calculated from an

optimized (100)-type surface structure in which doubly coordinated sites were protonated

and singly coordinated groups were singly protonated.

Implications of pK_a Predictions

The molecular scale picture for surface charge on gibbsite suggested by our pK_a

estimates is quite different from that of Hiemstra et al. (1999). Instead of singly

coordinated edge sites being solely responsible for surface charge, we show a number of

basal sites also participating in surface charging (Figure 4). Yet on average, the pK_a

estimates of Hiemstra et al. (1999) seem to be more or less in agreement with the

estimates that we calculated. Our average pK_a for the deprotonation of the $>Al_2OH_2^+$

basal sites (Eqn. 4) is 1.1 compared to their estimate of 0, and our average pK_a for the

deprotonation of the $>Al_2OH$ basal sites (Eqn. 5) is 10.3 compared to their estimate of

11.9. However, the problem with using average pK_a values to represent each site is that,

in reality, a surface consisting of identical site types may charge over a larger range of pH

conditions due to dynamic bond relaxation associated with changing protonation state.

In the case that some pK_a values occur within the pH range of interest but the average

occurs outside of that range, as is the case with our predicted pK_a values, some reactive

sites may be left out of the model. This could result in significant differences in model

predictions.

Another point that should be made about the predicted pK_a values in this study is

that we do not take them to be exact predictions. We discussed above some of the

problems associated with calculating reasonable *ab initio* surface structures. We expect

that some of the pK_a values we estimated from these structures include considerable

error. The magnitude of possible error is difficult to quantify but we believe that any of

the pK_a estimates could occur within about two log units of their predicted value.

However, we do believe that the pK_a values estimated here provide a more realistic range

of pK_a values for gibbsite surface sites than previous estimates.

MUSIC Modeling

The purpose of MUSIC models, as opposed to conventional surface complexation

models, is to experimentally or theoretically constrain important model parameters in

order to reduce the number of fitted parameters. In the remainder of this section, we will

propose an improved MUSIC model for gibbsite. Our results show that this new model is able to predict surface adsorption, not perfectly, but within a reasonable range for a number of titration data sets without re-introducing any of our estimated parameters as adjustable parameters. We will also compare the results of applying our model with results obtained from applying previous models to various titration data sets from several recent studies of gibbsite surfaces.

An improved MUSIC model for gibbsite

Using the pK_a estimates discussed above, we created a MUSIC model for the gibbsite sample of Jodin et al. (in press). We chose to model their surface charge data for several reasons. First, their surface area estimates were well constrained. They estimated the basal and edge surface area of their sample using both gas adsorption and the AFM methods described by Bickmore et al. (2002). Second, they used two-second time-resolved pH analysis to ensure adequate pH equilibration in their titrations. Solid concentrations in their titration experiments were about 32 g/L. The specific surface area of their sample was 4.5 m^2/g and edge surface area accounted for 37% of the total surface area.

All parameters used in this model are listed in Table 4. The only fitted parameters in the model are electrolyte binding constants and capacitances. All cation and anion binding constants were assumed to be equal in order to reduce the number of fitted parameters further. The fitted value for the binding constants is 0.49. The fitted values for basal and edge surface capacitances are 0.43 F/m^2 and 1.41 F/m^2, respectively. All other parameters, including pK_a values, site densities, and basal and edge surface area were constrained either theoretically or experimentally. In addition, we excluded the two

lowest pH values of each run for the regression analysis. We did this to avoid fitting our model through data points that had been potentially influenced by dissolution at low pH (Jodin et al., in press).

Figure 5 plots the surface charge vs. pH data from the titrations of Jodin et al. (in press) and our model predictions. One obvious characteristic of the model is that the surface charge predictions do not fit the titration data exactly. There are several reasons for this. First, Jodin et al. (in press) reported an increase in proton consumption at lower pH, causing hysteresis in the back-titration, indicating that dissolution may have a significant effect on gibbsite surface charge at low pH. Dissolution at low pH would cause surface charge curves to be higher than they would be in the absence of dissolution. Also, the imperfect fit between model predictions and titration data can be attributed to error in estimates of model parameters, specifically pK_a. We discussed above that some of the pK_a values we estimated from these structures likely include considerable error.

On the other hand, the model does predict several important surface-charging properties of gibbsite quite well. Specifically, the points of net zero proton charge (PZNPCs) and points of zero salt effect (PZSEs) do not coincide and the PZNPCs occur over a range instead of at a single pH value. The reason these characteristics are predicted by our model is that it consists of two spatially separated surfaces with very different charging behavior.

The PZNPC of a mineral is the pH at which the net charge due to proton adsorption/desorption at the mineral surface is equal to zero. In potentiometric titrations of solid phases lacking permanent structural charge, the PZNPC is typically assumed to be the same as the point of zero salt effect (PZSE), the pH at which suspensions of

24

varying ionic strengths have equal surface charge (McBride, 1994). Jodin et al. (in press) did not follow this convention. Instead, they allowed their sample to equilibriate with the pure salt solution and took the resulting pH as a good estimate of the sample's PZNPC (Gaboriaud and Ehrhardt, 2003). At the PZNPC of a mineral with essentially one type of surface, the salt effect is zero since the all surfaces are actually uncharged, or nearly so. However, this is not necessarily true for a mineral such as gibbsite, which has multiple surface types, each with a different PZNPC. In this case, the PZNPC for the sample is the pH at which the charge on the basal surface cancels out the charge on the edge surface, leaving a net charge of zero. Yet, since both surfaces are still charged at this point, salt effects on each surface still exist. In fact, for a gibbsite-like mineral, ionic strength affects the surface charge at every pH. As a result, solutions of different ionic strengths have different PZNPCs, and the PZNPCs do not necessarily coincide with the PZSE.

Another interesting difference between the titration data and the model is that titration data show three separate points of zero salt effect between the three curves (Figure 6a). Jodin et al. (2005) attributed these differences to experimental error. However, these differences may be real. As noted above, at least one gibbsite surface is always charged, regardless of pH. The magnitude of the total surface charge at each pH is, therefore, dependent on ionic strength and the resulting salt effects. As a result, titration curves for gibbsite at various ionic strengths should intersect at different pH values, not all at the same pH as would be the case for minerals with essentially a single type of surface. Although at the scale shown in Figure 5, the model titration curves appear to intersect at a single pH, closer inspection at a smaller scale reveals that the

model reproduces this phenomenon (Figure 6b). In addition, by adjusting pK_a values 1 or 2 log units, we were able to exaggerate the differences between PZSEs for each of the different ionic strength pairs so that they occurred over about 1.5 pH units, much like the data. This phenomenon is analogous to the charging behavior exhibited by mineral surfaces that have some permanent structural charge. On these surfaces, salt suppresses proton adsorption on permanent charge sites but promotes proton adsorption at pH-dependent charge sites. In such systems, unique PZSEs may not exist (McBride, 1994).

The variable PZNPC values predicted by the model are interesting considering that numerous studies of gibbsite surfaces based on potentiometric titrations and electrophoretic mobility have succeeded in constraining the PZNPC of gibbsite only over a fairly wide range (Figure 7). The PZNPC of gibbsite varies because it has multiple surfaces with different charging behavior, which cause it to behave in the same way as a composite oxide system. These systems consist of two component oxides of known PZNPC in the same solution. It has long been understood that the PZNPC of a composite oxide system (containing two component oxides) would occur between the PZNPCs of the component oxides. Studies have shown that the best way to predict a composite PZNPC is to use experimental titration data for each of the component oxides in a surface area weighted average (Parks, 1967; Kuo and Yen, 1987). In a gibbsite suspension, the two components in the system are the basal and edge surfaces. As such, the range of possible PZNPC values and exactly where the PZNPC for a given sample will occur within that range depends on several parameters. First, it depends on the PZNPC values of the basal and edge surfaces. Our model predicts the PZNPC for the basal and edge surfaces of gibbsite at pH 4.5 and 10.5, respectively. These PZNPC values define the

possible range of the composite PZNPC. If a hypothetical gibbsite sample were bounded

only by edge surfaces, it would have a PZNPC of 10.5. Similarly, if it were bounded

only by basal surfaces it would have a PZNPC of 4.5. However, real gibbsite samples are

bounded by both edge and basal surfaces. Therefore, the composite PZNPC would be

somewhere between 4.5 and 10.5 (Figure 8). Second, where the composite PZNPC

occurs within this range largely depends on how much o f each surface there is. A

sample with a high fraction of edge surface area will have a composite PZNPC closer to

the edge surface PZNPC of 10.5. On the other hand, a sample with a low fraction of edge

surface area will have a composite PZNPC closer to the basal surface PZNPC of 4.5.

Finally, the sensitivity of surface charge to changes in pH also affects the total PZNPC.

The surface with a greater sensitivity of surface charge to changes in pH will have a

greater effect on the composite PZNPC and cause the composite PZNPC to occur closer

to the PZNPC of that surface.

The implications of these points for our model of the titrations of Jodin et al. (in

press) are illustrated in Figure 8. As expected, the model PZNPC of the sample lies

between the PZNPCs of the basal and edge surfaces. In addition, the pH-sensitivity of

surface charge density (the slope of the curves) is much greater on the edge surface than

the basal surface. Because of this, the effect of the edge surface on the total PZNPC is

weighted more. As a result, the composite PZNPC is closer to the edge PZNPC than the

basal PZNPC even though the sample contains only 37% edge surface area.

On the other hand, Jodin et al. (in press) estimated pK_a values for gibbsite surface

sites using a different method (Table 5). They modified the MUSIC method by 1)

adjusting the number of available proton docking sites (see Eqn 2.), and 2) adjusting the

valence assigned to O-H bonds and weak hydrogen bonds based on spectroscopic evidence. However, they did not estimate a pK_a for the deprotonation of $>Al_2OH$, so Table 5 reports the original MUSIC method estimate of 11.9 (see Eqn. 5). Figure 9 plots surface charge vs. pH for their titration data and a MUSIC model we created using these pK_a and surface area estimates. Although their model fails to account for some of the surface charging phenomena accounted for by our model, it does a reasonable job of accounting for PZNPC and magnitude of surface charge. However, although the MUSIC method explicitly allows modelers to adjust the number of available proton docking sites on a surface O atom, there is no theoretical or experimental justification for doing so. In essence, this allows the modeler to adjust individual pK_a values by 4 log units in either direction in order to fit the data. *Ab initio* molecular dynamics simulations of solvated oxyacids have recently shown that the valence and number of H bonds to the O atoms varies with S_b and I (B.R. Bickmore and K.M. Rosso, unpublished data). This result is in complete agreement with our model pK_a prediction (Bickmore et al., 2004), but completely at odds with the MUSIC method. Thus, minor adjustments to the MUSIC method such as those made by Jodin et al. (in press) should probably be seen as nothing more than curve-fittting devices, rather than a reflection of molecular-scale reality.

Our model also accounts for the gibbsite titration data of Kavanagh et al. (1975). In order to maintain as much consistency as possible, fitted parameters were not re-fit to this data but are the same as listed in Table 4. In addition, we set the zero charge line (PZNPC) to the PZSE since that has been the conventional method for defining zero charge (McBride, 1994), and we suspect Kavanagh et al. (1975) used this method as well. Figure 10 plots surface charge vs. pH for the titration data of Kavanagh et al. (1975) and

our model predictions using two different estimates of percentage edge surface area. We created two models with different percentages of edge surface area to account for the range of possible values. The only previous edge surface area estimate for this sample (22%) used number-averaged particle dimensions (Hiemstra et al., 1999) based on powder XRD patterns. As we discussed above, number-averaging is a very unreliable method. For the first model, we used 18% edge surface area, which is the percent ESA on our sample H and is also equal to the lowest reported mass-normalized estimates for gibbsite ESA (Hiemstra et al., 1999). For the second model, we used 38% ESA, which is the percent ESA of our sample L and the percent ESA reported by Jodin et al. (2004) for their gibbsite sample.

The first model does not fit the data very well (Figure 10a). It predicts a PZSE of 8.3, significantly lower than the PZSE of 9.6 shown by the titration data. However, the slopes of the curves are similar. The second model, which assumes a greater percentage of edge surface area, fits the data quite well (Figure 10b). The predicted PZSE is 9.45 and the slopes of the curves are nearly identical. The better fit of the second model is consistent with the hypothesis that the percent ESA of this sample may have been closer to 38% than the previous estimate of 22% (Hiemstra et al., 1999). This is very likely because the previous estimate involved number-averaging, which has been shown to underestimate the fraction of ESA (see Table 1) (Bickmore et al., 2002; Jodin et al., 2004).

This data was also modeled by Hiemstra et al. (1999). The model predictions of Hiesmtra et al. (1999) seem to fit the titration data very well. However, there are a number of underlying problems. First, Hiemstra et al. (1999) were unable to account for

the magnitude of surface charge shown in the data of Kavangh et al. (1975) assuming only edge sites are reactive (i.e., only the reaction in Eqn. 6 was considered.). Instead, they assumed that singly coordinated defects existed on basal surfaces. In order to model the data, they spread the singly coordinated edge sites out over the total surface area and assumed the overall site density to be the average of basal (0 nm^{-2}) and edge (8.1 nm^{-2}) site densities. The first problem with this approach is that even if there are defects on the basal surfaces, there is no justification for lowering the site density on the edge surfaces to 4 nm^{-2}. This allows more protons to gather at the edge surfaces and build up a higher charge in the model than is probable in reality. In addition, although it is possible that defects, which replace doubly coordinated sites with singly coordinated sites, may exist on the basal surface, it may not be reasonable to suggest that they exist in great numbers. In order to determine how many defects would have to be present on the basal surface, we created a model using the same parameters as Hiemstra et al. (1999) but treated basal and edge surfaces separately. Our model showed that, in addition to the singly coordinated sites with a density of 8.1 nm^{-2} on the edge surfaces, singly coordinated sites would have to be present on the basal surfaces at a density of 4 nm^{-1}. Since the density of doubly coordinated sites on basal surfaces is 13.7 nm^{-2}, this would suggest that nearly 1/3 of basal sites would have to be defects.

In addition to modeling the titration data of Kavanagh et al. (1975), Hiemstra et al. (1999) also modeled their own titration data. Figure 11a plots surface charge vs. pH for titration data of Hiemstra et al. (1999) and model predictions from the same study. In this model, Hiemstra et al. (1999) excluded basal surfaces entirely, citing a lack of reactivity for these sites in the pH range of interest (see Eqns. 4-5). Instead, only edge

surfaces were considered. While their model did a reasonably good job of accounting for their titration data, our model was unable to do so. However, we believe that there are problems both with the collection of this titration data and with model assumptions. It is likely that the two-minute titration step times used by Hiemstra et al. (1999) to collect their titration data may not have been long enough. Recent studies have shown that the length of titration time steps has a significant influence on gibbsite surface charge data (Jodin et al., in press; Rosenqvist et al., 2002). Rosenqvist et al. (2002) were able to achieve magnitudes of surface charge similar to those of Hiemstra et al. (1999) using two-minute titration steps. However, when they increased the length of titration steps to between 8-14 hours, the resulting surface charge was about seven times greater (Rosenqvist et al., 2002). Jodin et al. (in press) pointed out that dissolution probably contributed to high surface charge of Rosenqvist et al. (2002), but also showed, using two-second time-resolved pH analysis, that 10-minute titration steps were necessary to insure adequate pH equilibration for their sample. The resulting surface charge using 10-minute titration steps was comparable to that of Kavanagh et al. (1975) and about four times greater than that of Hiemstra et al. (1999).

The length of titration time steps necessary to ensure pH equilibrium probably also depends on the number and size of gibbsite particles in suspension. Smaller particles and higher solid concentration might promote flocculation, which would obscure some of the reactive surface area. Thus, longer titration step times would be required, but this would also promote dissolution. Jodin et al. (in press) had larger particles (4.5 m^2/g) but used a higher solid concentration (32 g/L). Kavanagh et al. (1975), on the other hand, had much smaller particles (48 m^2/g) but used a lower solid concentration (5 g/L). For

each of these studies, titration step times of between 10 – 30 minutes were sufficient to ensure pH equilibration (see Rosenqvist et al., 2002). On the other hand, Hiemstra et al. (1999) performed titrations on small particles (40 m^2/g) and used a high solid concentration (30 g/L). With such small particles and high solid concentrations, there could have been significant flocculation in their suspensions. Thus, two-minute titration steps for their suspensions were likely not long enough. Rosenqvist et al. (2002) used small particles (29 m^2/g) and moderate solid concentration (12 g/L) in their suspensions. They tried to ensure pH equilibration by using 8-14 hour titration steps but such long titration step times probably promoted significant dissolution (Jodin et al., in press). In fact, Rosenqvist et al. (2002) reported spectroscopic evidence that new singly coordinated sites were being generated on their sample at low pH.

In addition, the model of Hiemstra et al. (1999) does not achieve such a good fit with titration data when gibbsite basal surfaces are included in the model. Even though basal surface pK_a values predicted by Hiemstra et al. (1999) are outside the pH range of interest, these sites would have some influence on surface charge. Figure 11b plots surface charge vs. pH for titration data of Hiemstra et al. (1999) and a model that accounts for basal surfaces, and treats basal and edge surfaces separately. While the magnitude of surface charge remains about the same, the addition of the basal surface causes several significant changes. The basal surface, which has a PZNPC of ~6 using the pK_a values from Eqns. 4-5, lowers the PZNPC. The added surface also creates the effect discussed above, which gives different ionic strengths different PZNPCs, and makes the PZNPCs different from the PZSE.

One recent study that correctly differentiated between gibbsite basal and edge surfaces in their MUSIC model was Rosenqvist et al. (2002). However, the surface charge calculated from their titration data was much too high to be accounted for using the model parameters of Hiemstra et al. (1999). In order to model their data, therefore, they added fitted values for log cation and anion binding constants of 8.49 and > 2.38, respectively. They also used a three-plane model, which employed fitted capacitance values for the inner and outer layers of 7.7 F/m^2 and 1.89 F/m^2, respectively. Their model achieved a good fit with their titration data, while our model was unable to do so. However, as mentioned above we believe that there were problems with the collection of this titration data. We also believe that there were problems with model assumptions. Even though Rosenqvist et al. (2002) used the pK_a values estimated by the MUSIC method of Hiesmtra et al. (1996) for acid-base reactions, their log K values for reactions involving background electrolyte ions (i.e., cation and anion binding constants were fitted. Fitting the values for electrolyte binding constants is not unusual in MUSIC modeling. However, the fitted constants of Rosenqvist et al. (2002) were so high that they allowed basal reactions involving ionic media to occur well within the pH range of interest and dominate model predictions. No experimental or theoretical justification for these adjustments was given. In fact, Rosenqvist et al. (2002) only used these fitted binding constant values on the basal surface. On the edge surface, they used a value of 0.1, based on the fitted values used by Hiemstra et al. (1999). Consequently, we believe that these adjustments were used only as curve-fitting devices. Finally, the capacitance value of 7.7 F/m2 used for the inner-sphere layer of this model is very unrealistic.

Capacitance is related to the average dielectric constant of the medium between two charged planes by the following equation

$$C = \frac{\varepsilon_r \varepsilon_0}{d} \qquad (9)$$

where ε_r is the dielectric constant of the medium, ε_0 is the permitivity of a vacuum (8.85 x 10^{-12} F/m), and d is the distance between the two planes. A reasonable capacitance should result in a value for ε_r that is between the dielectric constant of the solid and of bulk water (about 10 – 80 F/m^2) (Hiemstra et al., 1999). In the model of Rosenqvist et al. (2002), Na$^+$ ions formed inner-sphere complexes on the basal surface. Using Eqn. 9 and a distance equal to the ionic radius of Na$^+$ (0.14 nm), a capacitance of 7.7 F/m^2 results in a dielectric constant of 122, much higher than that of bulk water. Using the hydrated radius of Na$^+$ instead, results in a dielectric constant of 261. However, they did not comment on this value since the inner and outer layer fitted capacitances resulted in a total capacitance of 1.49 F/m^2 using the following equation

$$\frac{1}{C} = \frac{1}{C_1} + \frac{1}{C_2} \qquad (10)$$

where C, C_1, and C_2 are the total, inner layer, and outer layer capacitances, respectively. Using this definition, it is possible that physically unrealistic values for C_1 and C_2 can result in a physically reasonable value for C, as was the case for Rosenqvist et al. (2002).

CONCLUSIONS

Previous MUSIC models for gibbsite have relied on physically unrealistic assumptions and the re-introduction of adjustable parameters to fit their models to the data. This often results in a good fit; however, it does not provide a realistic picture of

surface reactivity at the molecular scale that can be applied to multiple titration data sets or gibbsite samples. We believe that this goal can be reasonably approximated by using the methods of surface area and pK_a estimation advocated here and in other recent studies (Bickmore et al., 2002; 2004; Jodin et al., 2004; in press). Discrepancies between model predictions and titration data that exist in the new model are likely due to error in titration data and pK_a prediction. Given the difficulty associated with calculating *ab initio* surface structures, we do not take the pK_a estimates made in this study to be exact. Rather, we believe that they exhibit a more realistic range than has been estimated previously. Advances in methods of calculating surface structures could improve the precision of these pK_a predictions and the surface charge predictions and of future MUSIC models.

REFERENCES

Bickmore B. R., Nagy K. L., Sandlin P. E., and Crater T. S. (2002) Quantifying surface areas of clays by atomic force microscopy. American Mineralogist 87, 780-783.

Bickmore B. R., Rosso K. M., Nagy K. L., Cygan R. T., and Tadanier C. J. (2003) Ab initio determination of edge surface structures for dioctahedreal 2:1 phyllosilicates: Implications for acid-base reactivity. Clays and Clay Minerals 51, 359-371.

Bickmore B. R., Tadanier C. J., Rosso K. M., Monn W. D., and Eggett D. L. (2004) Bond-Valence methods for pKa prediction: critical reanalysis and a new approach. Geochimica et Cosmochimica Acta 68, 2025-2042.

Brown I. D. and Altermatt D. (1985) Bond-valence parameters obtained from a systematic analysis of the inorganic crystal sructure database. Acta Crystallographica B41, 244-247.

Ducker W. A., Xu Z., Clarke D. R., and Israelachvili J. N. (1994) Forces between alumina surfaces in salt solutions: Non-DLVO forces and the implications for colloidal proccessing. Journal of the American Ceramic Society 77, 437-443.

Franks G. V. and Meagher L. (2003) The isoelectric points of sapphire crystals and alpha-alumina powder. Colloids and Surfaces A 214, 99-110.

Gaboriaud F. and Ehrhardt J. J. (2003) Effects of different crystal faces on the surface charge of colloidal goethite (alpha-FeOOH) particles: An experimental modeling study. Geochimica et Cosmochimica Acta 67(5), 967-983.

Hiemstra T., Van Riemsdijk W. H., and G.H. B. (1989) Multisite proton adsorption modeling at the solid/solution interface of (hydr)oxides: A new approach. I. Model description and evaluation of intrinsic reaction constants. Journal of Colloid and Interface Science 133, 91-104.

Hiemstra T., Venema P., and Van Riemsdijk W. H. (1996) Intrinsic proton affinity of reactive surface groups of metal (hydr)oxides: The bond valence principle. Journal of Colloid and Interface Science 184, 680-692.

Hiemstra T., Yong H., and Van Riemsdijk W. H. (1999) Interfacial charging phenomena of aluminum (hydr)oxides. Langmuir 15, 5942-5955.

Horn R. G., Clarke D. R., and Clarkson M. T. (1998) Direct measurement of surface forces between sapphire crystals in aqueous-solutions. Journal of Materials Research 3, 413-416.

Jodin M. C., Gaboriaud F., and Humbert B. (2004) Reprocussions of size heterogeneity on the measurement of specific surface areas of colloidal minerals: Combination of macroscopic and microscopic analyses. American Mineralogist 89, 1456-1462.

Kavanagh B. V., Posner A. M., and Quirk J. P. (1975) Effect of polymer adsorption on the properties of the electrical double layer. Discussions of the Faraday Society 59, 242-249.

Kosmulski M. (2003) Chemical Properties of Material Surfaces. Marcel Dekker.

Kresse G. and Furthmuller J. (1996) Efficient iterative schemes for ab initio total energy calculations using a plane-wave basis set. Physical Review B: Condensed Matter 54, 11169-11186.

Kuo J. F. and Yen T. F. (1987) Some aspects in predicting the point of zero charge of a composite oxide system. Journal of Colloid and Interface Science 121, 220-225.

Larson I., Drummond C. J., Chan D. Y. C., and Grieser F. (1997) Direct force measurements between silica and alumina. Langmuir 13, 2109-2112.

McBride M. B. (1994) Environmental Chemistry of Soils. Oxford University Press.

Meagher L., Maurdev G., and Gee M. L. (2002) Interaction forces between a bare silica surface and an alphi-alumina surface bearing adsorbed polyelectrolyte and surfactant. Langmuir 18, 2649-2657.

Parks G. A. (1967) Aqueous surface chemistry of oxides and complex oxide minerals. Isoelectric point and zero point of charge. In American Chemical Society Advances in Chemistry Series, Vol. 67 (ed. W. Stumm), pp. 121-160.

Pauling L. (1960) *The Nature of the Chemical Bond.* Cornell University Press, Ithaca.

Payne M. C., Teter M. P., Allen D. C., Arias T. A., and Joannopoulos J. D. (1992) Iterative minimization techniques for ab initio total-energy calculations: Molecular dynamics and conjugate gradients. Reviews of Modern Physics 64, 1045-1097.

Perdew J. P. and Wang Y. (1992) Accurate and simple analytic representation of the electron-gas correlation-energy. Physical Review B: Condensed Matter 45, 132444-13249.

Poeter E. P. and Hill M. C. (1998) Documentation of UCODE, A ComputerCode for Universal Inverse Modeling. In U.S. Geological Survey Water-Resources Investigations.

Rosenqvist J., Persson P., and Sjoberg S. (2002) Protonation and charging of nanosized

gibbsite (alpha-Al(OH)3) particles in aqueous suspension. Langmuir 18, 4598-4604.

Rosso K. M. (2001) Structure and reactivity of semiconducting mineral surfaces: Convergence of molecular modeling and experiment. In Reviews in Mineralogy and Geochemistry, Vol. 42 (ed. R. T. Cygan and J. D. Kubicki), pp. 199-271. Mineralogical Society of America.

Rustad J. R. and Felmy A. R. (2005) The influence of edge sites on the development of surface charge on geothite nanoparticles: A molecular dynamics investigation. Geochimica et Cosmochimica Acta 69, 1405-1411.

Rustad J. R., Felmy A. R., and Bylaska E. J. (2003) Molecular simulation of the magnetite-water interface. Geochimica et Cosmochimica Acta 67, 1001-1016.

Stack A. G., Higgins S. R., and Eggleston C. M. (2001) Point of zero charge of a corundum-water interface probed with optical Second Harmonic Generation (SHG) and Atomic Force Microscopy (AFM): New approaches to oxide surface charge. Geochimica et Cosmochimica Acta 65, 3055 - 3065.

Vanderbilt D. (1990) Soft self-consistent pseudopotentials in a generalized eigenvalue formalism. Physical Review B: Condensed Matter 41, 7892-7895.

Westall J. C. (1982) FITEQL, pp. A computer program for the determination of chemical equilibrium constants from experimental data. Department of Chemistry, University of Oregon.

White J. A. and Bird D. M. (1994) Implementation of gradient-corrected exchange-correlation potentials in Car-Parrinello total energy calculations. Physical Review B: Condensed Matter 50, 4954-4957.

TABLES

Table 1. SSA estimates from various studies using various methods.

Study	Sample	BET (m^2/g)	Other Methods (m^2/g)	% Edge Surface Area
This Study	H	37.7	40.8[a]	18%
	L	45.9	43.6[a]	37%
Hiemstra et al. (1999)	GH2	40.3	86.7[b]	23%
	GL1	40.8	51.2[b]	50%
Rosenqvist et al. (2002)		29.5	91[c]	9%
Jodin et al. (2004)			4[d], 4.5[a]	37%[d], 31%[a]

[a] estimated with AFM and computerized image analysis routines that include mass-normalization and corrections for microtopography (Bickmore et al., 2002).
[b] estimated using TEM and platinum shadowing, and mass-normalization.
[c] estimated using AFM and number-averaged particle dimensions.
[d] estimated using Kr-adsorption and infrared spectroscopy.

Table 2. SSA estimates for samples H and L using BET, number-averaged surface area from AFM images (ASA), mass-normalized surface area from AFM images (MNSA), and bottom-corrected, mass-normalized surface area from AFM images (BCMNSA). Number-averaging (ASA) significantly overestimates SSA while mass-normalization without corrections for microtopography on particle bottoms (MNSA) underestimates SSA. When the bottom correction is added (BCMNSA), BET surface area estimates are approximated within experimental error.

Sample	BET (m^2/g)	ASA (m^2/g)	MNSA (m^2/g)	BCMNSA (m^2/g)
H	37.7	174.4	22	40.8
L	45.9	97.9	38.9	43.6

Table 3. pK_a values estimated by applying the bond-valence method of Bickmore et al. (2004) to gibbsite (001) and (100) surface structure cacluated via *ab initio* methods. The six sites for basal reactions are based on the six functional groups present on our optimized basal surface. Our optimized edge surface contained only two singly coordinated sites so only two pK_a values were estimated for that reaction.

Site Specific pK_a Estimates						
Reaction	*Site Number*					
	1	*2*	*3*	*4*	*5*	*6*
$>Al_2OH_2^+ = >Al_2OH + H^+$	-2.3	-1.6	-5.1	-0.4	5.2	10.8
$>Al_2OH = >Al_2O^- + H^+$	3.9	11.4	3.2	8.8	14.4	20
$>AlOH_2^{+1/2} = >AlOH^{-1/2} + H^+$	10.7	10.4				

Table 4. Parameters used in our new MUSIC model for gibbsite.

| Reactions | Site Number | | | | | |
	1	2	3	4	5	6
	Log K					
$>Al_2OH + H^+ = >Al_2OH_2^+$	-2.3	-1.6	-5.1	-0.4	5.2	10.8
$>Al_2OH = >Al_2O^- + H^+$	-3.9	-11.4	-3.2	-8.6	-14.2	-19.8
$>Al_2OH + H^+ + Cl^- = >Al_2OH_2^+ --- Cl^-$	-1.8	-1.1	-4.6	0.1	5.7	11.3
$>Al_2OH = >Al_2O^- --- Na^+ + H^+$	-3.4	-10.9	3.7	-8.1	-13.7	-19.3
$>AlOH^{-1/2} + H^+ = >AlOH_2^{+1/2}$	10.7	10.4				
$>AlOH^{-1/2} + H^+ + Cl^- = >AlOH_2^{+1/2} --- Cl^-$	11.2	10.9				
$>AlOH^{-1/2} + Na^+ = >AlOH_2^{-1/2} --- Na^+$	0.5	0.5				

Fitted Parameters	
Basal Capacitance	0.43 F/m^2
Edge Capacitance	1.41 F/m^2

Table 5. pK_a estimates by Jodin et al. (in press) and parameters used to create a MUSIC model.

Reaction	pK_a
>Al$_2$OH$_2$$^+$ = >Al$_2$OH + H$^+$	4
>Al$_2$OH = >Al$_2$O$^-$ + H$^+$	11.9[a]
>AlOH$_2$$^{+1/2}$ = >AlOH$^{-1/2}$ + H$^+$	7.9
Fitted Parameters	
Basal Capacitance	0.5 F/m^2
Edge Capacitance	1.8 F/m^2
Electrolyte Binding Constant	log K = 0.5

[a] pK_a estimate made by Hiemstra et al. (1999), since an estimate for this reaction was not made by Jodin et al. (in press).
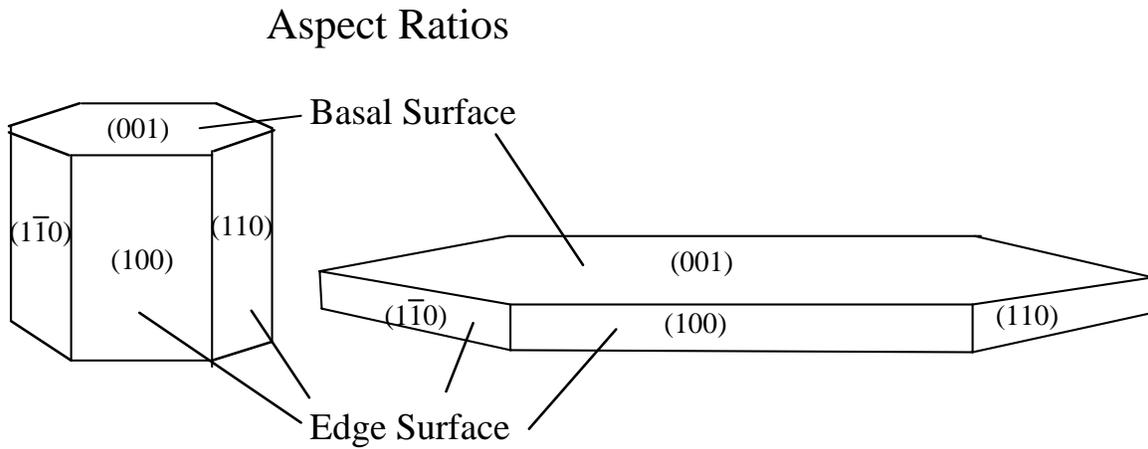
Aspect Ratios

Figure 1. Diagram showing particles with different aspect ratios. Gibbsite particles are platy and pseudo-hexagonal. Basal (001)-type surfaces consist of only $>Al_2OH$ sites. Edge (100)-type and (110)-type surfaces consist of both $>Al_2OH$ and $>AlOH^{-1/2}$ or $>AlOH_2^{+1/2}$ sites in equal densities. Samples crystallized at low temperatures should exhibit a higher ratio of edge to basal surface area.
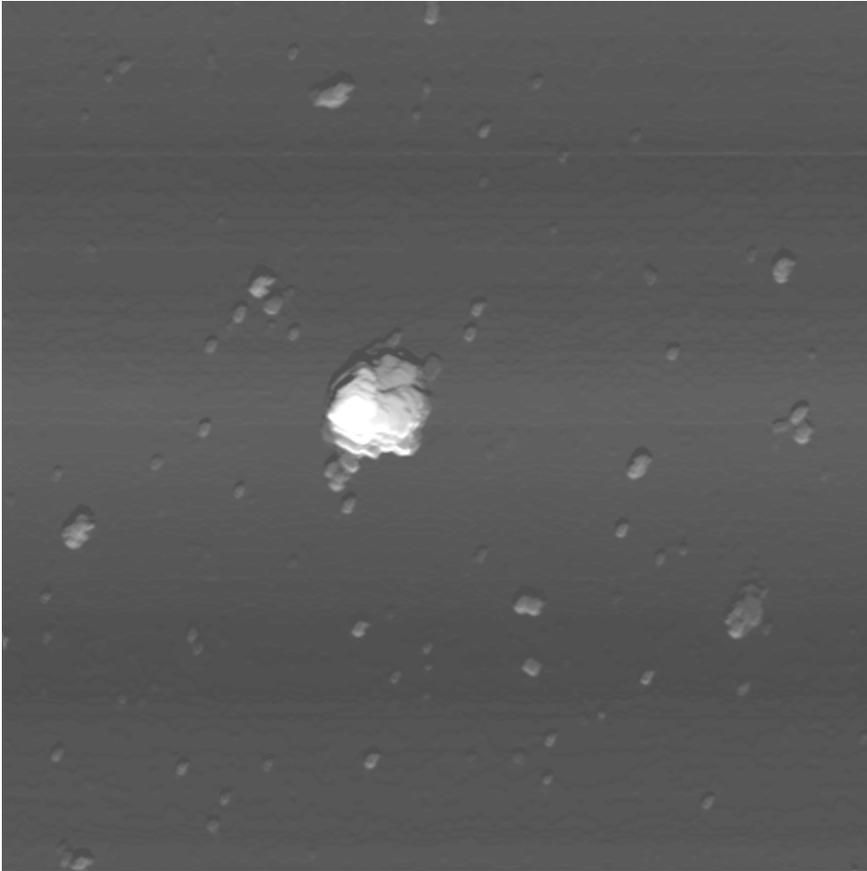
Figure 2. AFM image of sample L with a shadowing routine added to enhance
topography. This image demonstrates the heterogeneous nature of the sample with
respect to particle size, with the smaller particles outnumbering the larger ones.
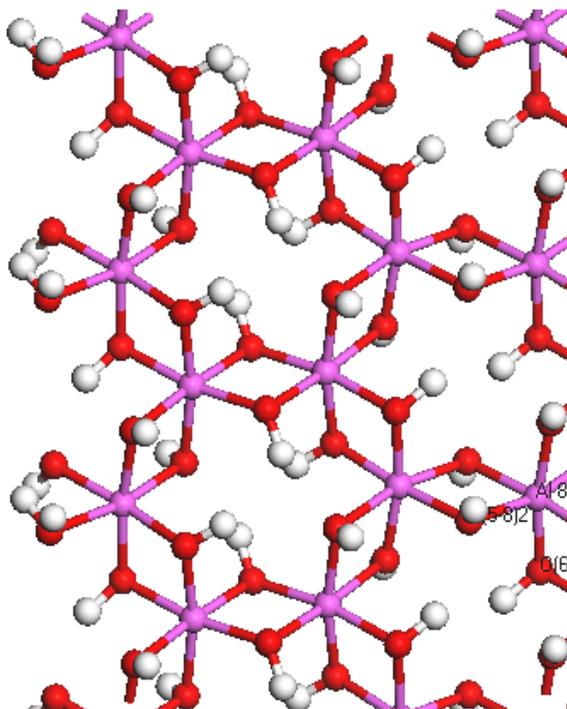
Figure 3. Gibbsite (110)-type edge surface that shows >Al$_2$OH groups set deeper into the surface than >AlOH$^{-1/2}$ and >AlOH$_2$$^{+1/2}$. As a result of this positioning, they are probably inaccessible to water molecules and assumed not to participate in acid/base reactions.
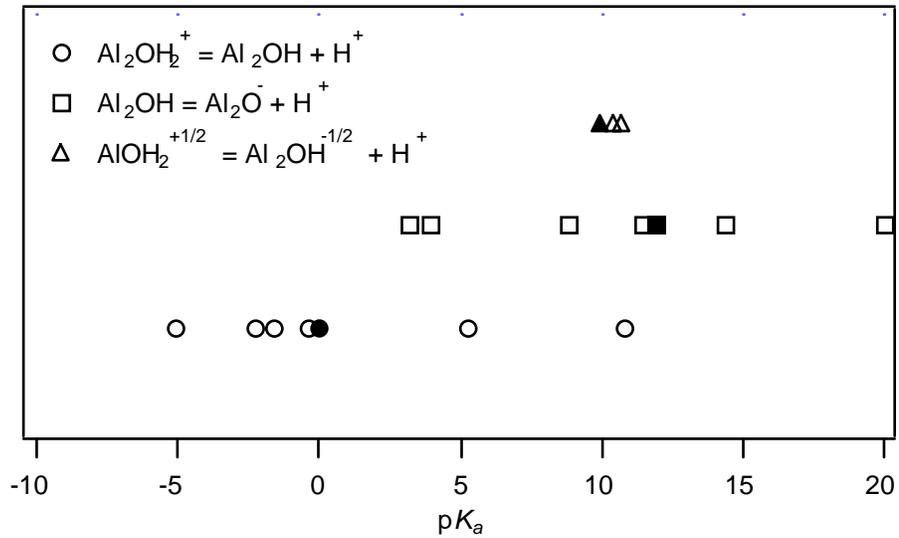
Figure 4. Estimated pK_a values for gibbsite surface reactions. Open markers are estimates from this study and opaque markers are estimates from Hiemstra et al. (1999) using the MUSIC method. The estimates of Hiemstra et al. (1999) seem to approximate an average of estimates from this study. However, based on the estimates of Hiemstra et al. (1999), no basal sites are reactive in the pH 3-11 range, while estimates from this study suggest that at least some are reactive in this range.
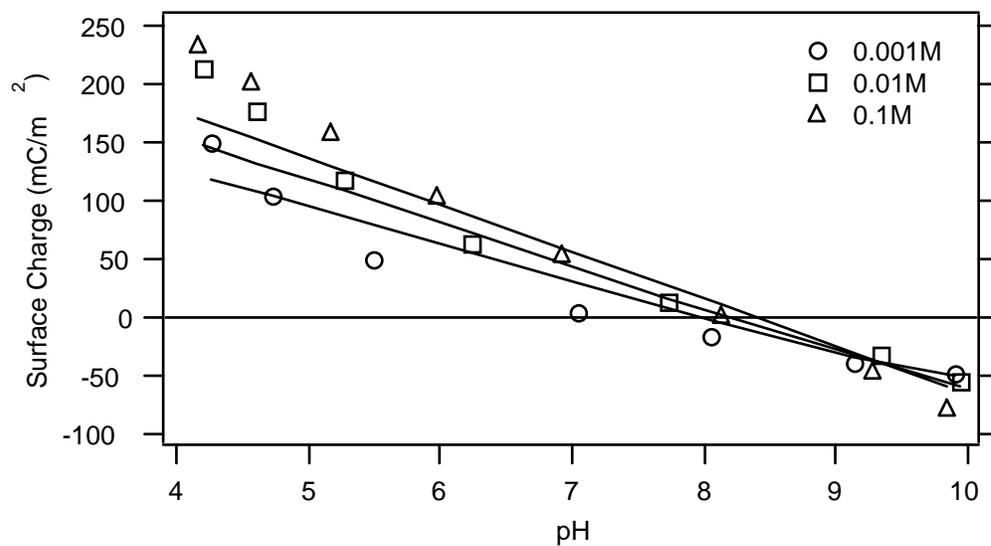
Figure 5. Gibbsite potentiometric titration data of Jodin et al. (in press) and model predictions from our new model. The fit is not exact, due to error associated with titration data and pK_a estimates; however, magnitude of surface charge, PZNPC, and PZSE are accounted for quite well.
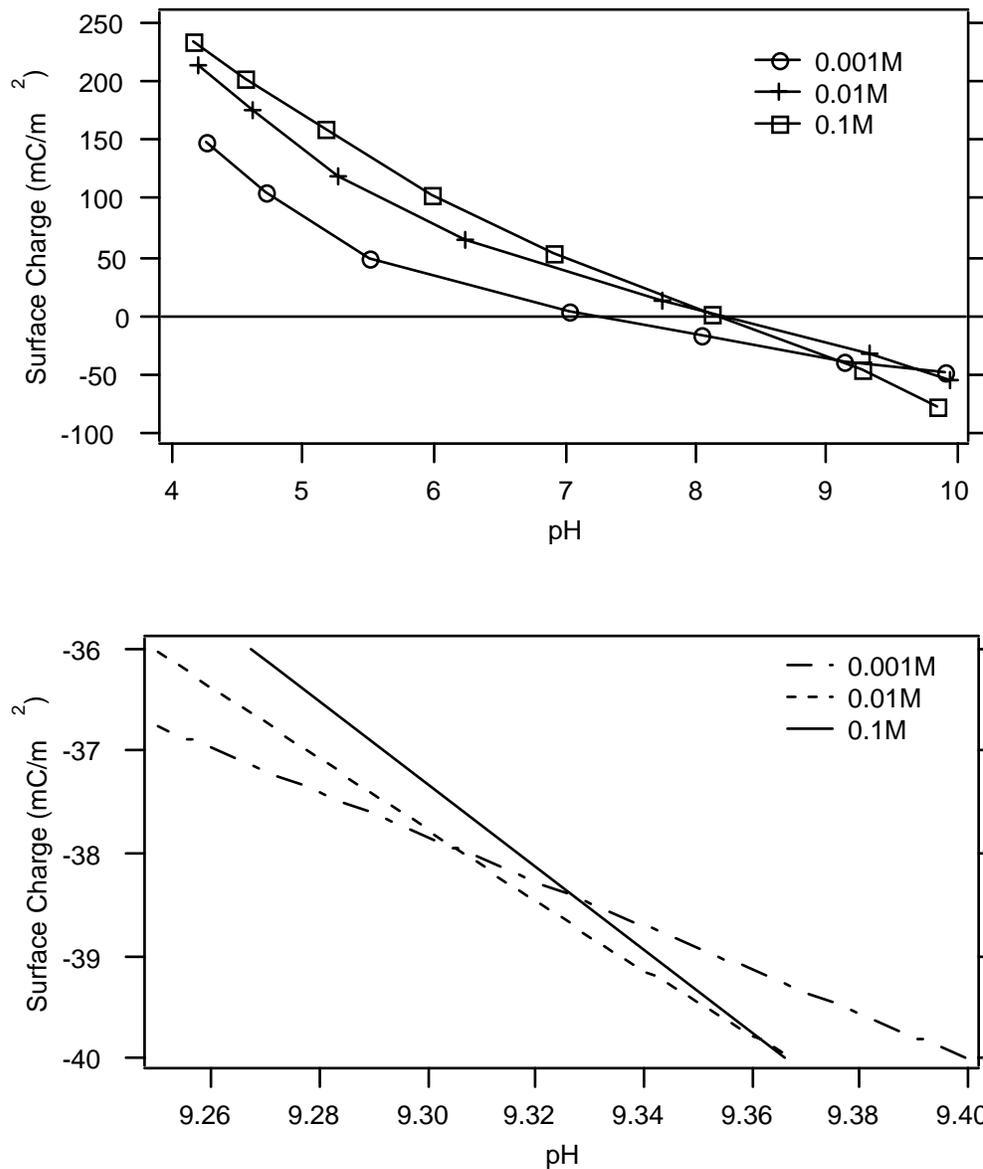
Figure 6. (a) The gibbsite potentiometric titration data of Jodin et al. (in press) shown here does not exhibit a unique PZSE. (b) On a smaller scale than shown in Figure 5, our model predicts this phenomenon. Adjusting pK_a values 1 or 2 log units can also enhance this effect.
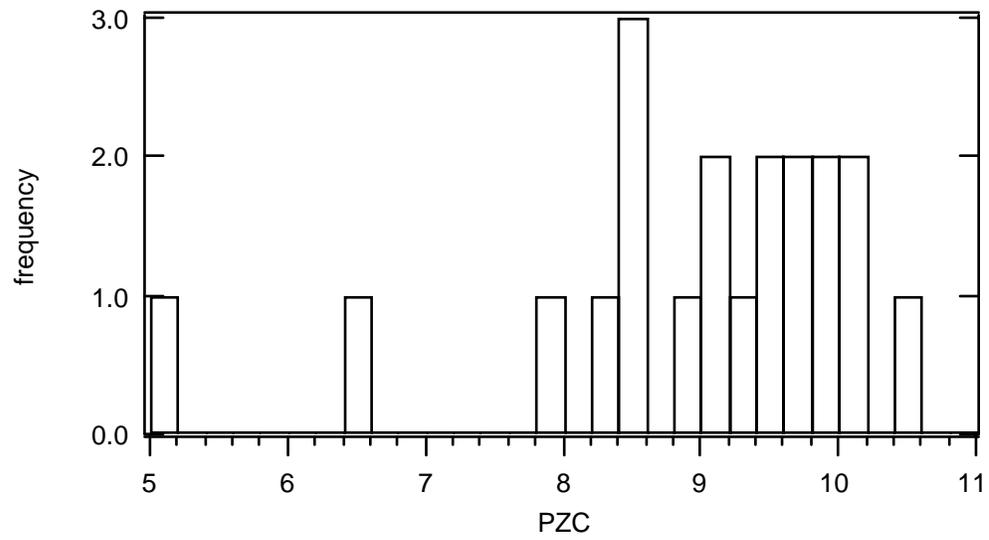
Figure 7. Reported values for the PZC of gibbsite (estimated from PZSE and isoelectric point) from Kosmulski, (2001).
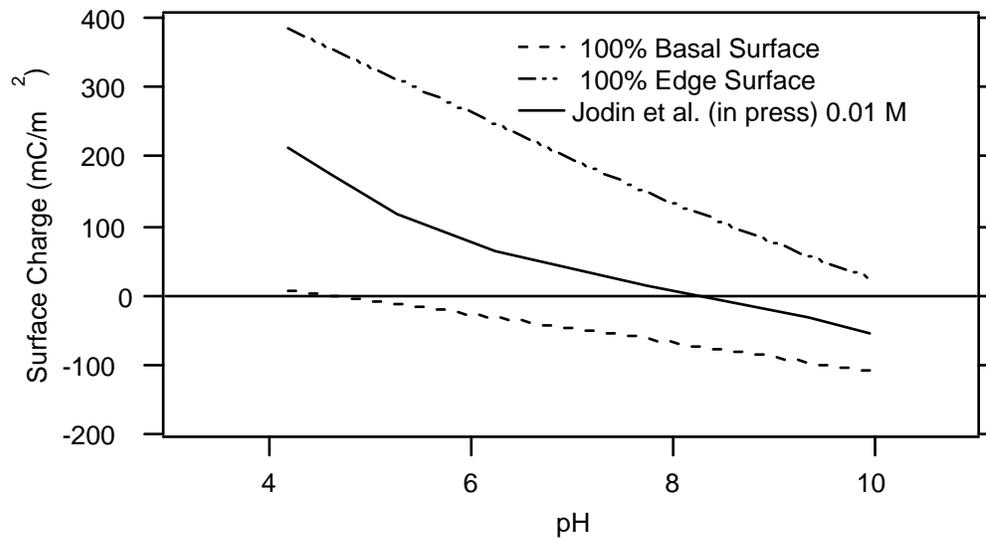
Figure 8. Gibbsite potentiometric titration data (0.01 M NaCl) from Jodin et al. (in press) along with model predictions for hypothetical gibbsite samples bounded exclusively by basal or edge surfaces. Ideally, the PZNPCs of the hypothetical samples should determine the range of possible values for a composite PZNPC, while the slopes of the curves and relative amount of each surface present should determine the exact value of the PZNPC.
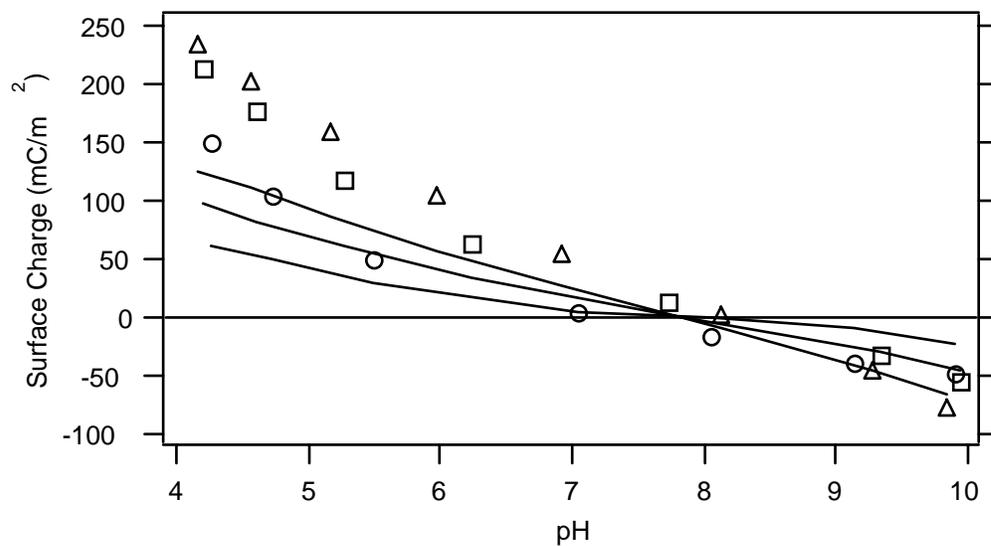
Figure 9. Gibbsite potentiometric titration data of Jodin et al. (in press) and a model using pK_a values predicted in the same study. These pKa values were estimated by adjusting the number of proton docking sites available on O atoms and the valence assigned to O-H and weak H bonds.
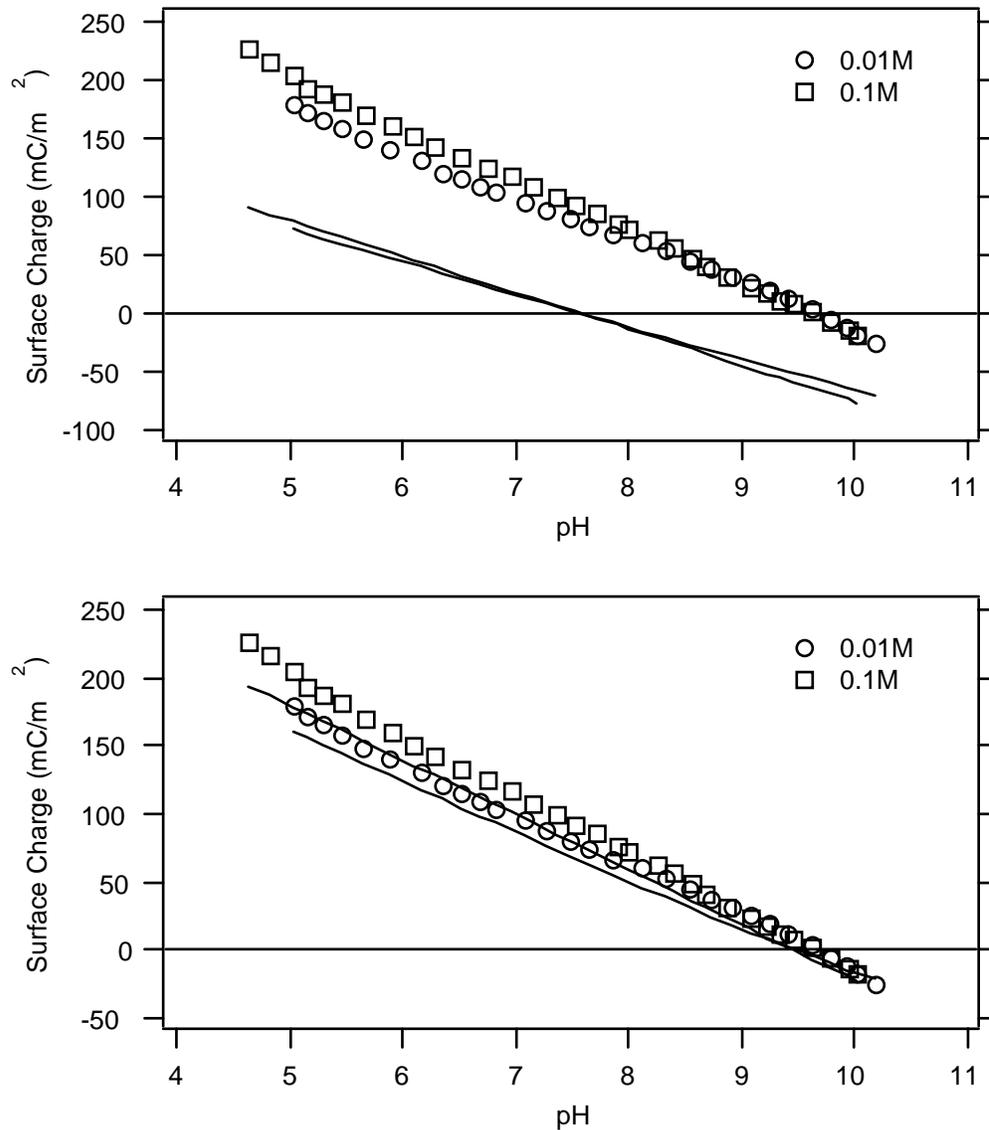
Figure 10. (a) Gibbsite potentiometric titration data from Kavanagh et al. (1975) and a model created using pK_a predictions from this study. Capacitance values were 0.43 F/m^2 for the basal surface and 1.41 F/m^2 for the edge surface. Percent ESA was 18%. Although the slopes of the charging curves are similar, the PZSE is significantly different. This suggests that the ESA assumption might be inaccurate. (b) The same data and model as (a) but using 37% ESA. The better fit of this model is consistent with the hypothesis that the ESA of the sample of Kavanagh et al. (1975) might have been closer to 37%.
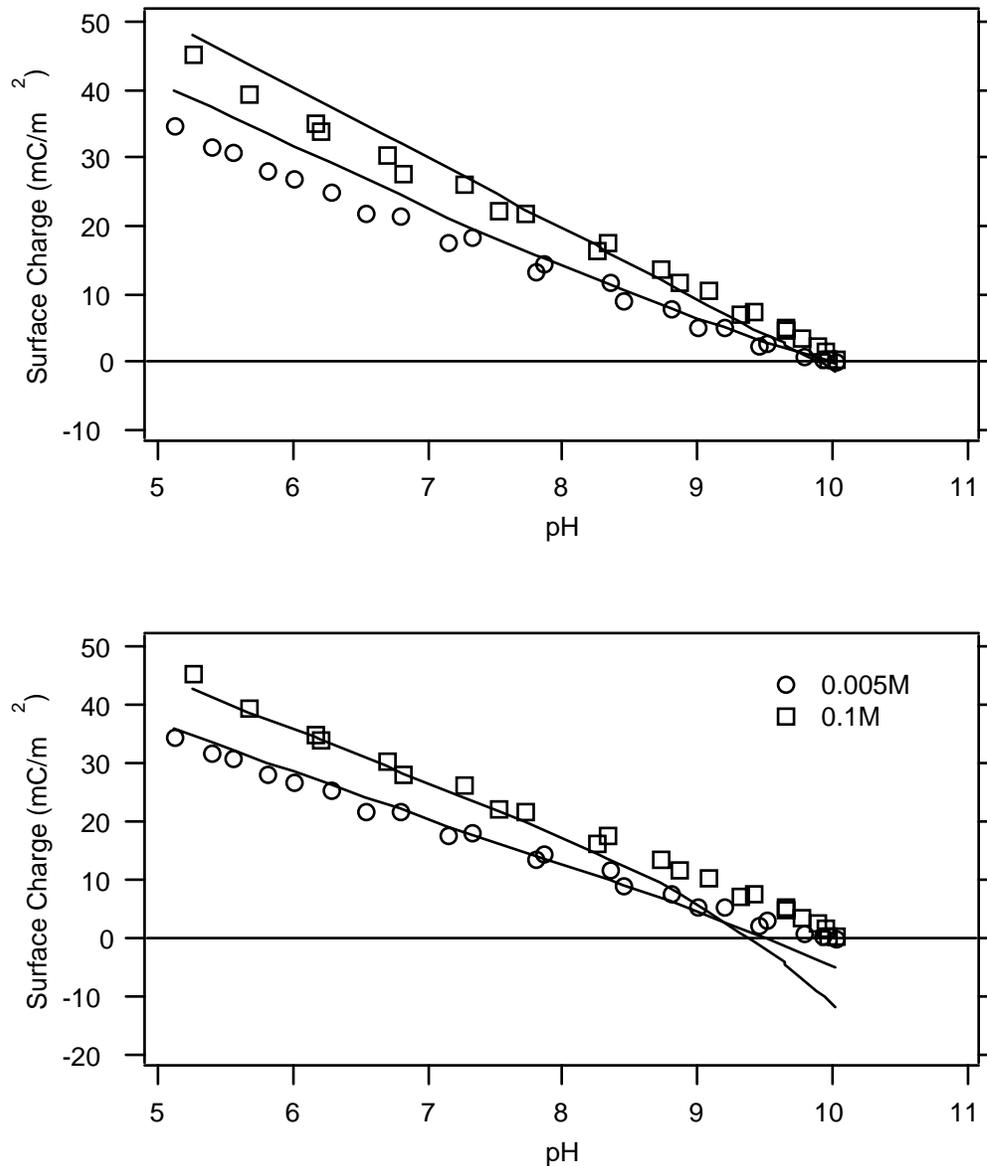
Figure 11. (a) Gibbsite potentiometric titration data and model predictions from Hiemstra et al. (1999) for their sample GH2. Although the model seems to fit the data quite well, short titration step times and unrealistic model assumptions lead us to believe that the model may not provide an accurate description of surface reactivity. (b) Model created after Hiemstra et al. (1999) and modified to account for both edge and basal surfaces. Hiemstra et al. (1999) suggested that basal sites would not be reactive in this pH range; however, as shown here, they would be sufficiently reactive to cause a lower predicted PZNPC and a non-unique PZSE.